

## Generalized Trio Coherent States

A. S.-F. Obada,<sup>1</sup> H. H. Salah,<sup>2</sup> M. A. Darwish,<sup>3</sup> and E. M. Khalil<sup>1,4</sup>

Received November 22, 2004; accepted March 30, 2005

---

Generalized trio coherent states are made by superposing a number of trio coherent states. They possess inherent nonclassical properties such as sub-Poissonian distribution and violation of Cauchy-Schwarz inequalities. Their phase distribution in the framework of the Pegg and Barnett theory is discussed. We study the interaction of the radiation field prepared in a generalized trio coherent state with an atom in a superposition coherent state in the rotating wave approximation. We investigate the time dependence of the sub-Poissonian distribution and the violation of Cauchy-Schwarz inequalities for such a system. General conclusions reached are illustrated by numerical results.

---

**KEY WORDS:** trio coherent; sub-Poissonian; Cauchy-Schwarz inequality; phase distribution.

### 1. INTRODUCTION

The concept of coherent states (CSs) was introduced by Glauber (1963). Since then they attained an important position in quantum optics. This is because the CSs not only have physical content but also yield a very useful representation. The usual CSs introduced by Glauber are eigenstates of the annihilation operator  $\hat{a}$  of the harmonic oscillator. Based on Glauber's work, the even and odd CSs were introduced (Dodonov *et al.*, 1974). The even (odd) CSs are the symmetric (antisymmetric) combination of the CSs. They are two orthonormalized eigenstates of  $(\hat{a}^2)$  the square of the annihilation operator  $\hat{a}$  and essentially have two kinds of nonclassical effects: the even CS has a squeezing but no antibunching effect, while the odd CS has an antibunching but no squeezing effect (Hillery, 1987; Xia and Guo, 1989). In quantum optics, Schrödinger-cat states are usually described as superpositions of different coherent states (Buzek and Knight, 1995), as coherent

<sup>1</sup>Mathematics Department, Faculty of Science, Al-Azhar University Nasr City 11884, Cairo, Egypt.

<sup>2</sup>Physics Department, Faculty of Science (girls), Al-Azhar University Nasr City, Cairo, Egypt.

<sup>3</sup>Faculty of Education, Suez Canal University at Al-Arish, Egypt.

<sup>4</sup>To whom correspondence should be addressed at Mathematics Department, Faculty of Science, Al-Azhar University Nasr City 11884, Cairo, Egypt; e-mail: eied73@hotmail.com.

states are the closest quantum states to a classical description of a field of definite complex amplitude. Specifically, the archetype of a Schrödinger-cat state is given by the superposition  $|\Psi\rangle_{SC} = N[|\alpha\rangle + \exp(i\phi)|-\alpha\rangle]$ , where  $|\alpha\rangle$  is a coherent state of the single-mode quantized field and  $N$  is a normalization coefficient. In particular, these states are referred to the even, odd and Yurke-Stoler (Yurke and Stoler, 1986) coherent states when  $\phi = 0, \pi$  and  $\frac{\pi}{2}$ , respectively. They have been extensively studied and shown to exhibit nonclassical properties such as squeezing and sub-Poissonian statistics (Buzek and Knight, 1995).

Gerry and Grobe (1995) proposed a two-mode generalization of Schrödinger-cat states defined as superpositions of different pair-coherent states (PCS). For two annihilation operators  $\hat{a}_1$  and  $\hat{a}_2$ , a pair-coherent state  $|\zeta, q\rangle$  is defined as an eigenstate of both the pair annihilation operator  $\hat{a}_1\hat{a}_2$  for the two modes, and the photon number difference between the two modes (i.e., Bhaumik *et al.*, 1976):

$$\begin{aligned} \hat{a}_1\hat{a}_2|\zeta, q\rangle &= \zeta|\zeta, q\rangle \\ (\hat{a}_2^\dagger\hat{a}_2 - \hat{a}_1^\dagger\hat{a}_1)|\zeta, q\rangle &= q|\zeta, q\rangle \end{aligned} \tag{1}$$

where  $\zeta$  is a complex number and  $q$  is the parameter, which is a fixed integer.

Then it can be seen that the pair-coherent state takes the form

$$|\zeta, q\rangle = N_q \sum_{n=0}^{\infty} \frac{\zeta^n}{\sqrt{n!(n+q)!}} |n, n+q\rangle \tag{2}$$

with

$$N_q = \frac{1}{\sqrt{\sum_{n=0}^{\infty} \frac{|\zeta|^{2n}}{n!(n+q)!}}} = [|\zeta|^{-q} I_q(2|\zeta|)]^{-\frac{1}{2}}, \tag{3}$$

where  $N_q$  is the normalization constant ( $I_q$  is the modified Bessel function of the first kind of order  $q$ ).

The correlated two-mode Schrödinger-cat states  $|\zeta, q, \phi\rangle$  are defined as superpositions of two (PCS) separated in phase by  $\pi$  (Gerry and Grobe, 1995):

$$|\zeta, q, \phi\rangle = N_\phi [|\zeta, q\rangle + \exp(i\phi)|-\zeta, q\rangle], \tag{4}$$

where the normalization constant  $N_\phi$  is given by

$$N_\phi = \frac{1}{\sqrt{2}} \left[ 1 + N_q^2 \cos \phi \sum_{n=0}^{\infty} \frac{(-1)^n |\zeta|^{2n}}{n!(n+q)!} \right]^{-\frac{1}{2}}, \tag{5}$$

It is easy to verify that the states  $|\zeta, q, \phi\rangle$  are eigenstates of the operator  $(\hat{a}_1\hat{a}_2)^2$  with eigenvalue  $\zeta^2$ .

Recently, in addition to various kinds of known non-classical states (Glauber, 1963), a new one called a trio coherent state (TCS) has been introduced (Nguyen and Truong, 2002; Nguyen, 2002; Yi *et al.*, 2004; Nguyen and Truong, 2002).

These states have been investigated and the even and odd trio coherent states have been studied for antibunching and Cauchy-Schwarz inequalities (Nguyen and Truong, 2002).

Our target in the present paper is a generalization of the trio coherent state, which in turn is a generalized Schrödinger-cat state. The paper is organized as follows: In Section 2 we present the correlated trio coherent state and the generalized trio coherent state (GTCS). Some statistical quantities are computed for a GTCS representation: the second order correlation function in Section 3, Cauchy-Schwarz inequalities in Section 4, the phase distribution in Section 5. In Section 6 we study the interaction of the radiation field prepared in generalized trio coherent states with atom in the superposition coherent state in rotating wave approximation (RWA). In Sections 7 and 8 we study the temporal behavior of the sub-Poissonian distribution and violation of Cauchy-Schwarz inequalities respectively. Finally conclusions are summarized in Section 9.

**2. GENERALIZED TRIO COHERENT STATE (GTCS)**

We consider the trio coherent state TCS, which is a generalization of pair-coherent state. The TCS is eigenstate for the commuting operators  $\hat{a}_1\hat{a}_2\hat{a}_3$ ,  $\hat{P} = \hat{n}_2 - \hat{n}_1$  and  $\hat{Q} = \hat{n}_3 - \hat{n}_1$  with  $\hat{n}_{1(2,3)} = \hat{a}_1^\dagger\hat{a}_1(\hat{a}_2^\dagger\hat{a}_2, \hat{a}_3^\dagger\hat{a}_3)$  and  $\hat{a}_1(\hat{a}_2\hat{a}_3)$  the bosonic annihilation operator for mode 1(2, 3), i.e.

$$\hat{a}_1\hat{a}_2\hat{a}_3|\zeta, p, q\rangle = \zeta|\zeta, p, q\rangle, \tag{6}$$

$$\hat{P}|\zeta, p, q\rangle = p|\zeta, p, q\rangle, \tag{7}$$

$$\hat{Q}|\zeta, p, q\rangle = q|\zeta, p, q\rangle, \tag{8}$$

where  $\zeta = r \exp(i\phi)$  with real  $r, \phi$  is the complex eigenvalue and  $p, q$  are non-negative integers. The TCS is defined as follows:

$$|\zeta, p, q\rangle = N_{p,q} \sum_{n=0}^{\infty} \frac{\zeta^n}{\sqrt{n!(n+p)!(n+q)!}} |n, n+p, n+q\rangle, \tag{9}$$

with

$$N_{p,q} = \frac{1}{\sqrt{\sum_{n=0}^{\infty} \frac{|\zeta|^{2n}}{n!(n+p)!(n+q)!}}}, \tag{10}$$

where  $N_{p,q}$  is the normalization constant. we define a generalized class of trio-coherent states in a similar way to the generalized Schrödinger-cat states, as follows:

$$|\zeta, p, q, k\rangle_j = N_{p,q,j} \sum_{n=0}^{\infty} \frac{\zeta^{kn+j}}{\sqrt{(kn+j)!(kn+p+j)!(kn+q+j)!}} \times |kn+j, kn+p+j, kn+q+j\rangle, \tag{11}$$

where  $N_{p,q,j}$  is given by

$$N_{p,q,j} = \frac{1}{\sqrt{\sum_{n=0}^{\infty} \frac{|\zeta|^{2(kn+j)}}{(kn+j)!(kn+p+j)!(kn+q+j)!}}}, \quad 0 \leq j \leq k \tag{12}$$

The states  $|\zeta, p, q, k\rangle_j$  are eigenstates of the operators  $(\hat{a}_1\hat{a}_2\hat{a}_3)^k$ ,  $\hat{P}$  and  $\hat{Q}$  (Yi *et al.*, 2004). When we take  $k = 2$  we get the even and odd trio coherent states of (Nguyen and Truong, 2002).

### 3. SUB-POISSONIAN DISTRIBUTION

We devote the present section to consider an example of the nonclassical effects that is the phenomenon of sub-Poissonian distribution. This phenomenon can be measured by photon detectors based on photoelectric effect. The importance of the study comes up as a result of several applications, e.g. in the gravitational wave detector and quantum nondemolition measurement, which can be generated in semiconductor lasers (Yamamoto and Machida, 1987) and in the microwave region using masers operating in the microscopic regime (Remoe *et al.*, 1990). It is well known that, sub-Poissonian statistics is characterized by the fact that the variance of the photon number  $\langle(\Delta\hat{n}_i(t))^2\rangle$  is less than the average photon number  $\langle\hat{a}_i^\dagger(t)\hat{a}_i(t)\rangle = \langle\hat{n}_i(t)\rangle$ . This can be expressed by means of the normalized second-order correlation function (Loundon, 1983) as follows. A mode  $x$  in a quantum state  $|\zeta, p, q, j\rangle$  is said to be sub-Poissonian if

$$g_x^2(0) = \frac{\langle\zeta, p, q, j|\hat{n}_x(\hat{n}_x - 1)|\zeta, p, q, j\rangle}{\langle\zeta, p, q, j|\hat{n}_x|\zeta, p, q, j\rangle^2} < 1, \tag{13}$$

where

$$\begin{aligned} &\langle\zeta, p, q, k|\hat{n}_x(\hat{n}_x - 1)|\zeta, p, q, k\rangle \\ &= |N_{p,q,j}|^2 \sum_{n=0}^{\infty} \frac{|\zeta|^{2(kn+j)}(kn+z_x+j)(kn+z_x+j-1)}{(kn+j)!(kn+p+j)!(kn+q+j)!}, \\ &x = 1, 2, 3 \end{aligned} \tag{14}$$

and

$$\begin{aligned} \langle\zeta, p, q, k|\hat{n}_x|\zeta, p, q, k\rangle &= |N_{p,q,j}|^2 \sum_{n=0}^{\infty} \frac{|\zeta|^{2(kn+j)}(kn+z_x+j)}{(kn+j)!(kn+p+j)!(kn+q+j)!}, \\ dx &= 1, 2, 3 \end{aligned} \tag{15}$$

The number  $z_i$  are set as follows: For the first mode  $z_1 = 0$ , the second mode  $z_2 = p$  and third mode  $z_3 = q$ . The function  $g_x^2(0)$  determined by (13) serves

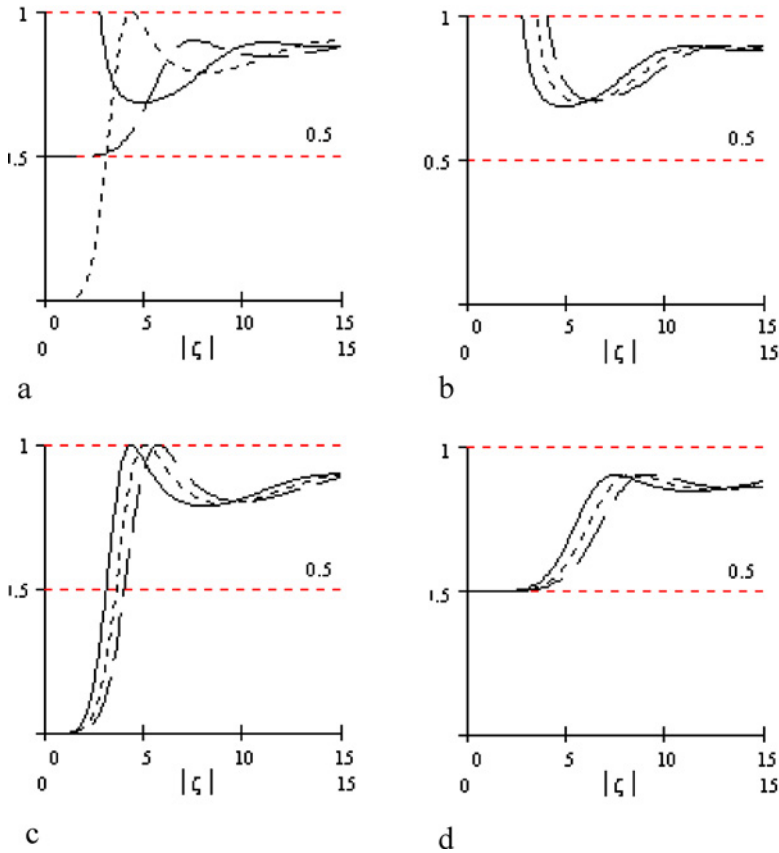


**Fig. 1.** The sub-Poissonian function  $g_1^2(\zeta)$  for mode 1 as function of  $|\zeta|$  in the GTCSs with  $k = 3$ , (a) for  $q = p = 0$  the solid curve for  $j = 0$ , the dot curve for  $j = 1$  and the ddot curve for  $j = 2$ , (b) for  $j = 0$ ,  $q = 0$  the solid curve for  $p = 0$ , the dot curve for  $p = 1$  and the ddot curve for  $p = 2$ , (c) same as b but  $j = 1$ , (d) same as b but  $j = 2$ .

as a measure of the deviation from the Poisson distribution that corresponds to  $g_x^2(0) = 1$ . If  $g_x^2(0) < 1 (> 1)$ , the field is called sub (super)-Poissonian.

In Fig. 1(a), the second-order correlation function  $g_1^2(0)$  for mode 1, given by (13), is plotted against  $|\zeta|$  for  $p = q = 0$  and  $k = 3$  (i.e.,  $j = 0, 1, 2$ ). This figure exhibits the very striking quantum nature of the generated field. For mode 1, we found that the distribution function starts to be sub-Poissonian  $g_1^2(0) < 1$  at small values of  $|\zeta|$  for  $j = 1$  and  $j = 2$  which is started from 0.5, but for  $j = 0$  a super-Poissonian behavior ( $g_1^2(0) > 1$ ) is presented. At some value of  $|\zeta|$  the state with  $j = 1$  becomes Poissonian ( $g_x^2(0) = 1$ ) while the state with  $j = 2$  becomes more favorable for sub-Poissonian than that with  $j = 0$ . The sub-Poissonian level

is worst, best and intermediate for the state  $j = 0$  at different values of  $|\zeta|$ , while the sub-Poissonian level of the other states with  $j = 1$  and  $j = 2$  are equal. The sub-Poissonian level oscillates in all states over a wide range of  $|\zeta|$ . We notice that the function  $g_x^2(0)$  in general shows oscillatory behavior until it becomes almost stable with  $|\zeta|$  increased.

The behavior of  $g_1^2(0)$  changes qualitatively, depending on the parameters  $p$  and  $q$  as seen in Fig. 1(b)–(d). As the parameters are increased the generalized trio coherent states (GTCSs) is shifting to the higher  $|\zeta|$  side. It can be noted that an inverse picture arises twice at different values of  $|\zeta|$  for each state. For  $j = 0$  changes the distribution from super-Poissonian to sub-Poissonian. While the interval of super-Poissonian increases as the parameter  $p$  is increased (see Fig. 1(b)). A significant result is that, for  $j \geq 1$  at small range of  $|\zeta|$  the sub-Poissonian level increases with increasing the parameter  $p$  (see Fig. 1(c) and (d)). There is a noticeable difference between  $j = 1$  and  $j = 2$ . For  $j = 1$  an almost ideal sub-Poissonian is achievable at very small values of  $|\zeta|$ . The distribution of this state changes from sub-Poissonian to Poissonian and then changes again to sub-Poissonian (see Fig. 1(c)). For  $j > 1$  the curves are shifted up to 0.5 and an ideal sub-Poissonian can never be reached. The sub-Poissonian behavior persists for the complete range of  $\zeta$  (see Fig. 1(d)).

The  $g_2^2(0)$  function for mode 2 and mode 1 are symmetric in case  $p = q = 0$  (see Fig. 1(a)). With increasing parameter  $p$  for state  $j = 0$  all curves are shifted toward small values of  $|\zeta|$  (see Fig. 2(a)). For states  $j \geq 1$  there appears to be a difference between mode 1 and mode 2. At  $j = 1$  for  $p = 0$ , the function  $g_2^2(0)$  emerges from zero, while for  $p \geq 1$  it starts from a non-zero value. For  $\zeta = 0$  the function  $g_2^2(0)$  has the limits  $0, 0.5, \frac{6}{9}$ , for  $p = 0, 1, 2$ , respectively, as observed in Fig. 2(b). For  $j = 2$  all curves are shifted up with increasing  $p$ , such that the  $g_2^2(0)$  equals  $0.5, \frac{6}{9}, \frac{3}{4}$ , for  $p = 0, 1, 2$ , respectively see Fig. 2(c). In addition,  $g_2^2(0)$  function becomes more sensitive to increasing the parameter  $p$ .

#### 4. CAUCHY-SCHWARZ INEQUALITY VIOLATION

The Cauchy-Schwarz inequality (Nguyen and Truong, 2002) is defined as

$$\begin{aligned} & \langle \zeta, p, q, k | \hat{n}_x (\hat{n}_x - 1) | \zeta, p, q, k \rangle \langle \zeta, p, q, k | \hat{n}_y (\hat{n}_y - 1) | \zeta, p, q, k \rangle \\ & \geq \langle \zeta, p, q, k | \hat{n}_x \hat{n}_y | \zeta, p, q, k \rangle^2 \end{aligned} \tag{16}$$

We shall examine the scaled Cauchy-Schwarz inequalities in our GTCs, which are determined by

$$F_{xy}(\zeta) = \frac{\langle \zeta, p, q, k | \hat{n}_x (\hat{n}_x - 1) | \zeta, p, q, k \rangle \langle \zeta, p, q, k | \hat{n}_y (\hat{n}_y - 1) | \zeta, p, q, k \rangle}{\langle \zeta, p, q, k | \hat{n}_x \hat{n}_y | \zeta, p, q, k \rangle^2}, \tag{17}$$

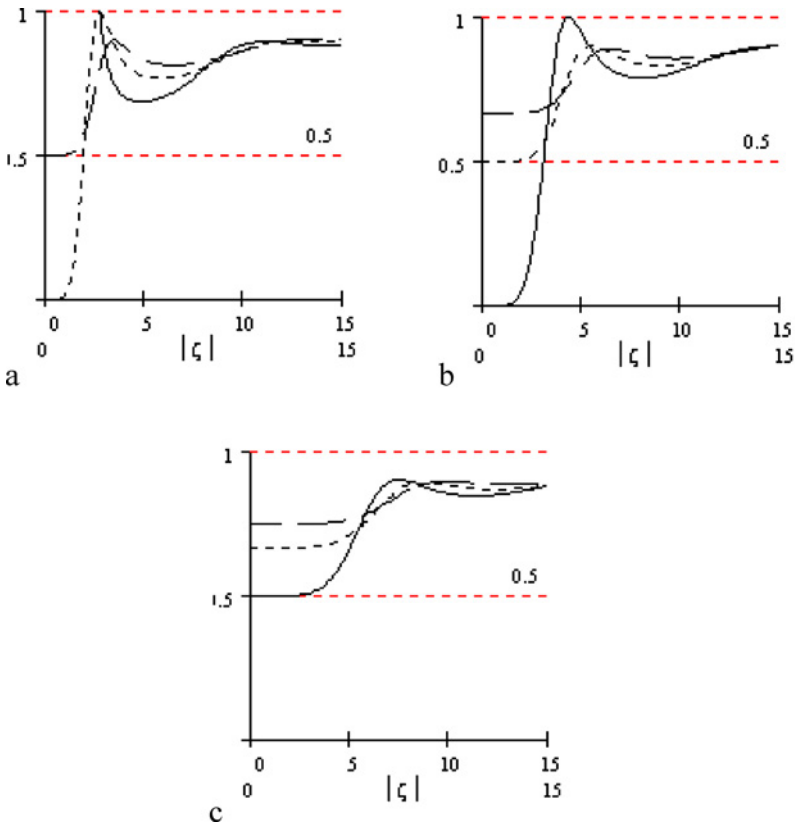


Fig. 2. Same as Fig. 1 but for mode 2.

The inequality (16) is violated if the function  $F_{xy}$  is less than unity. For that purpose we need to calculate the expectation values appearing in (17). Those in the numerator were already known from (14) and those in the denominator are calculated to be generally for  $k = 3$  (i.e.,  $j = 0, 1, 2$ ).

$$\langle \zeta, p, q, k | \hat{n}_x \hat{n}_y | \zeta, p, q, k \rangle = |N_{p,q,j}|^2 \sum_{n=0}^{\infty} \frac{\zeta^{2kn+2j} (kn + z_x + j)(kn + z_y + j)}{(kn + j)!(kn + p + j)!(kn + q + j)!},$$

$x, y = 1, 2, 3$  (18)

The numbers  $z_i$  are defined as  $z_i$  defined after Equation (15). The Cauchy-Schwarz inequality in the GTCs is clearly seen in Fig. 3 for the pair (2, 3) and  $k = 3$ . For state  $j = 0$  with a fixed  $q = 0$ , full violation starting from non-zero if  $p = 0, 1$

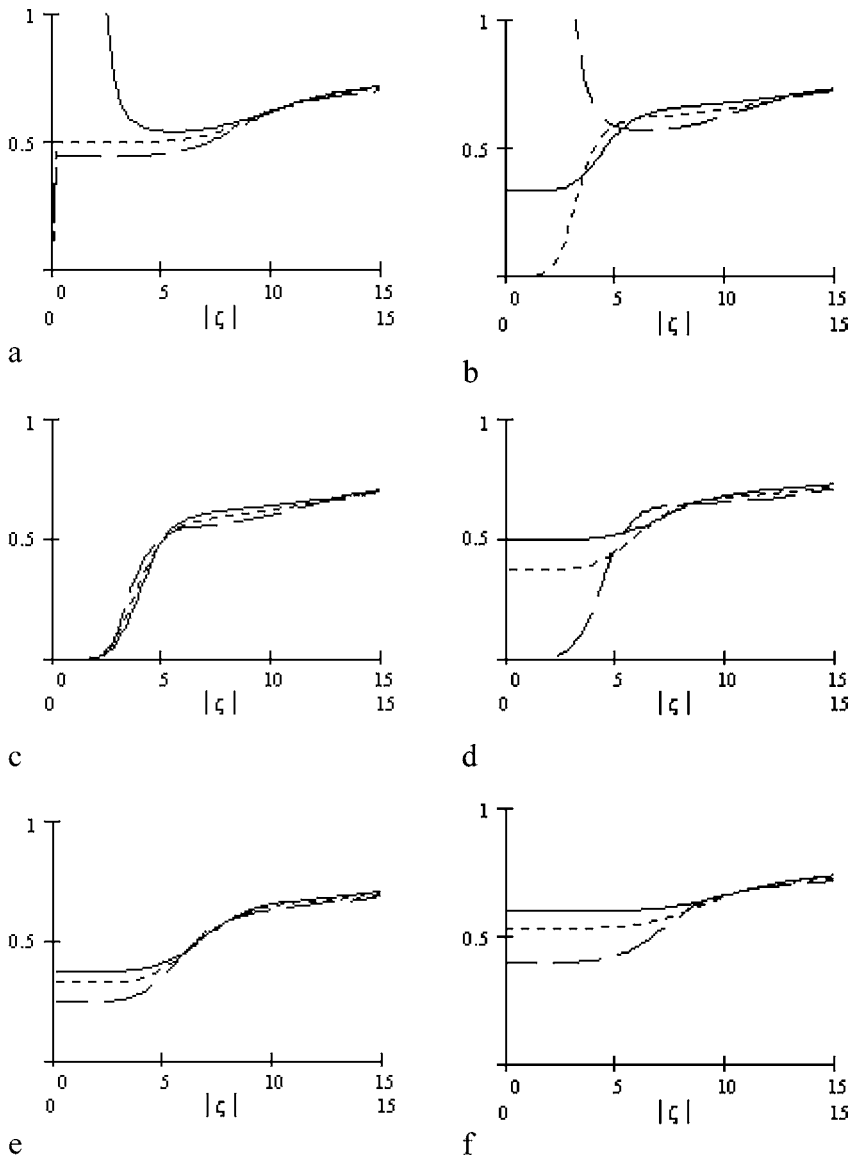


**Fig. 3.**  $F_{23}$  as function of  $|\zeta|$  and  $k = 3$ , (a) for  $j = 0$  and fixed  $q = 0$  the solid curve for  $p = 2$ , the dot curve for  $p = 1$  and the ddot curve for  $p = 0$ , (b) same as (a) but  $q = 3$ , (c) same as (a) but  $j = 1$ , (d) same as (a) but  $j = 1$  and  $q = 3$ , (e) same as (a) but  $j = 2$ , (f) same as (a) but  $j = 2$  and  $q = 3$ .



**Table I.** The Initial Values of the Function  $F_{23}(0)$  for the Pair (2,3)

		$p = 0$	$p = 1$	$p = 2$
$j = 0$	$q = 0$	0	0	$\infty$
	$q = 3$	$\infty$	0	$\frac{1}{3}$
$j = 1$	$q = 0$	0	0	0
	$q = 3$	0	$\frac{3}{8}$	$\frac{1}{2}$
$j = 2$	$q = 0$	$\frac{1}{4}$	$\frac{1}{3}$	$\frac{3}{8}$
	$q = 3$	$\frac{2}{5}$	$\frac{8}{15}$	$\frac{3}{5}$

and partially violated if  $p = 2$  (a partial violation means that  $F_{23} > 1$  at small  $|\zeta|$  and then becomes less than unity for large  $|\zeta|$ ) as in Fig. 3(a) (Yi *et al.*, 2004).

The Cauchy-Schwarz inequality in the GTCS for initial values are summarized in Table I. For fixed  $q = 3$ , full violation starting from zero if  $p = 1$ , nonzero if  $p = 2$ . At  $p = 0$ , the violation is weaker (stronger) at small  $|\zeta|$  (larger  $|\zeta|$ )-region, as seen in Fig. 3(b). If  $j \geq 1$  all curves are always violating with fixed value of  $q$  (see Fig. 3(c)–(f)). For  $j = 1$  the violation is independent of  $p$  at  $q = 0$  (Fig. 3(c)). For large fixed  $q$  value, the violation depends on  $p$  at small  $|\zeta|$  region. For  $j = 2$  the inequality is violated weakly for larger values of  $q$  (Fig. 3(e) and (f)).

Symmetry is present between the pair (2, 3) and (1, 2) with fixed value of  $q = 0$  and  $p = 0, 1, 2$  for the states [i.e.,  $j = 0, 1, 2$ ] see (Fig. 3(a), (c), and (e)). In Fig. 3(a) we see that all curves are partial violation but in Fig. 3(b) all curves are full violation starting from zero and in Fig. 3(c) full violation starting from a non-zero value. On the other hand for fixed  $p = 3$  and  $k = 3$  the violation is almost dependent of  $q$  see Fig. 4(a)–(c).

### 5. PHASE DISTRIBUTION

In the present section we shall discuss the phase distribution to study the effect of the parametric amplifier on the present system. For this reason it is convenient to use the phase distribution formalism introduced by Barnett and Pegg (Loundon, 1983; Pegg and Barnett, 1988; Pegg and Barnett, 1997; Barnett and Pegg, 1989; Special issue on, 1993). It is well known that the phase operator is defined as the projection operator on a particular phase state multiplied by the corresponding value of the phase. Therefore one can find that the Pegg-Barnett phases distribution function  $P(\theta_1, \theta_2, \theta_3, \zeta)$  is given by special issue on (1993):

$$\begin{aligned}
 &P(\theta_1, \theta_2, \theta_3, \zeta) = \\
 &\frac{|N_{p,q,j}|^2}{(2\pi)^3} \sum_{n,m} |kn + j, kn + p + j, kn + q + j\rangle \langle km + j, km + p + j, km + q + j| \\
 &\times \frac{\zeta^{kn+j} \zeta^{*km+j} \exp[i(kn - km)\theta_1 + i(kn - km)\theta_2 + i(kn - km)\theta_3]}{\sqrt{(kn + j)!(kn + p + j)!(kn + q + j)!(km + j)!(km + p + j)!(km + q + j)!}}. \quad (19)
 \end{aligned}$$

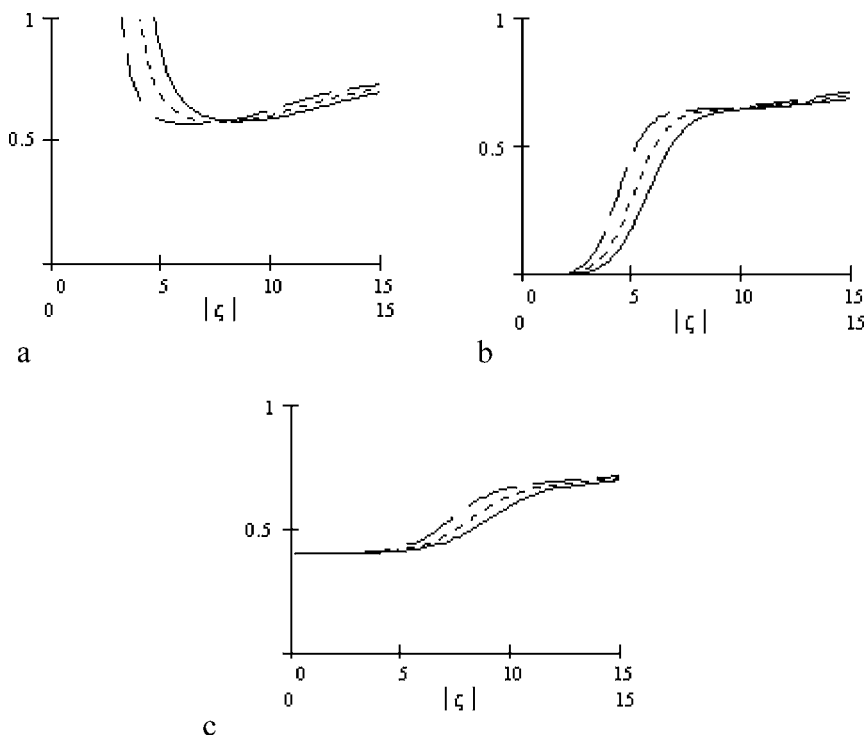


**Fig. 4.**  $F_{12}$  as function of  $|\zeta|$  and  $k = 3$ , (a)- for  $j = 0, p = 3$  the solid curve for  $q = 2$ , the dot curve for  $q = 1$  and the dot-dot curve for  $q = 0$ , (b)- same as (a) but  $j = 1$ , (c)- same as (a) but  $j = 2$ .

Now let us apply this definition to the case in which the generalized correlated trio-coherent state is taken into consideration. Therefore from Equation (19) the phases distribution function can be written as

$$P(\theta, \zeta) = \frac{|N_{p,q,j}|^2}{(2\pi)^3} \left| \sum_n \frac{\zeta^{kn+j} \exp[ikn\theta]}{\sqrt{(kn+j)!(kn+p+j)!(kn+q+j)!}} \right|^2, \quad -\pi \leq \theta \leq \pi \tag{20}$$

where  $\theta = \theta_1 + \theta_2 + \theta_3$ . In figure (5), we have plotted the phase distribution of GTCS as a function of  $(\theta, \zeta)$  for  $k = 3, 0 \leq j \leq 2$  and for fixed the parameters  $q = p = 0$ . At  $\zeta = 0$ , no information about the phase of the state as the phase distribution function acquires the value  $\frac{1}{(2\pi)^3}$ . As  $j$  increases we note that, the interval of the loss of information about the phase is increased. But for large values of  $|\zeta|$  the phase starts to develop three-peak symmetric around  $\theta = 0$ . For the case of  $j = 0$  the value of the peak lowers slightly by increasing  $|\zeta|$  then after

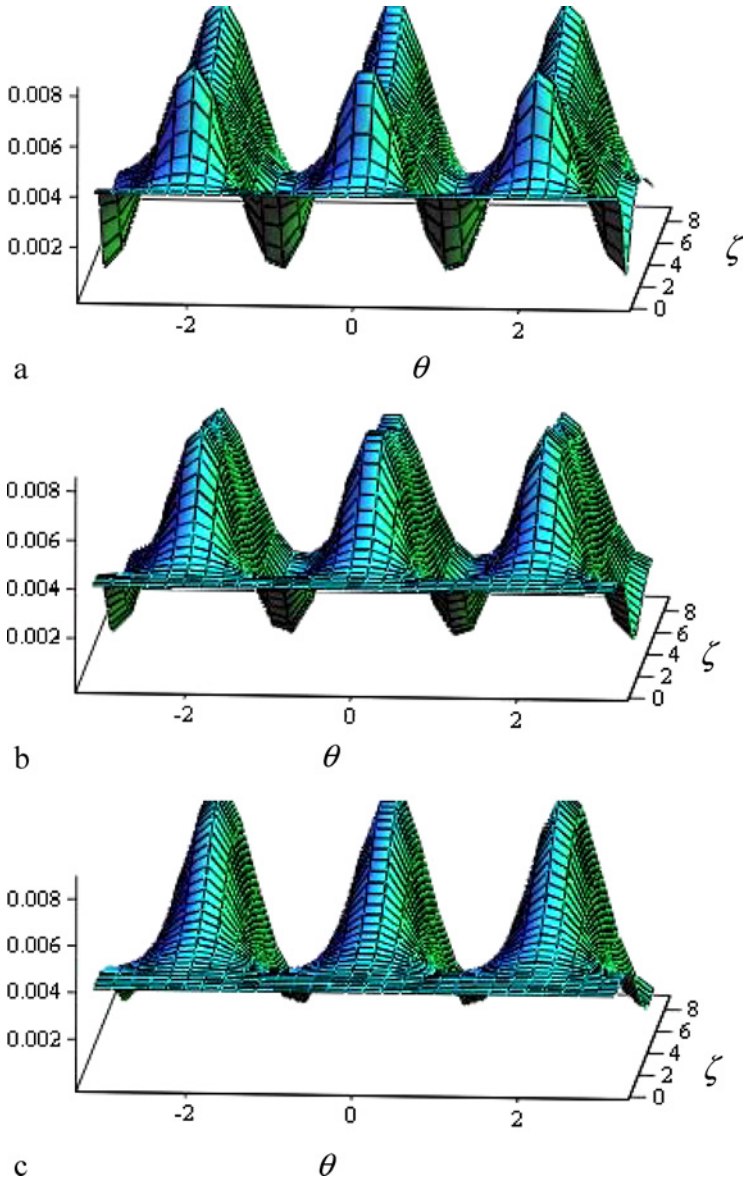


Fig. 5. The phase distribution  $P(\theta, \zeta)$  as function of  $\theta$  and  $|\zeta|$ ,  $p = q = 0, k = 3$  (a) for  $j = 0$ , (b)  $j = 1$ , (c)-  $j = 2$ .

that it starts increasing (Fig. 5(a)). This slight lowering is noticed also for  $j = 1$  (Fig. 5(b)). However for the case of  $j = 2$  this lowering is not observed for the range of  $|\zeta|$  considered (Fig. 5(c)). Changing the parameters  $q$  and  $p$  to the values other than zero results in extending the interval of no information about the phase.

### 6. MODEL AND SOLUTION

In the following we shall consider a Hamiltonian model that consists of three modes interacting with a two-level particle (atom or trapped ion). The quantized radiation field is considered in the rotating wave approximation frame considering that the interaction is nonlinear with the three modes of the cavity field. Then the Hamiltonian that describes such a system can be written as ( $\hbar = 1$ ),

$$\hat{H} = \omega_1 \hat{S}_{11} + \omega_2 \hat{S}_{22} + \sum_{j=1}^3 \Omega_j \hat{n}_j + \lambda[(\hat{a}_1 \hat{a}_2 \hat{a}_3)^k \hat{S}_{12} + (\hat{a}_1^\dagger \hat{a}_2^\dagger \hat{a}_3^\dagger)^k \hat{S}_{21}] \quad (21)$$

where  $\Omega_j$  and  $\omega_j$  are the frequency of the  $j$ th mode of the field and the energy of the  $j$ th level of the atom, while  $\hat{a}_j$  and  $(\hat{a}_j^\dagger)$  are annihilation and (creation) operators for the  $j$ th mode of the cavity field which obey the commutation relation  $[\hat{a}_i, \hat{a}_j^\dagger] = \delta_{ij}$ ,  $k$  is the multiplicity and  $\lambda$  is the effective coupling constant. The  $\hat{S}_{ij}$  operators are the generators of the group  $U(2)$  which satisfy the following commutation relation (Yoo and Eberly, 1985).

$$[\hat{S}_{ij}, \hat{S}_{lm}] = \hat{S}_{im} \delta_{jl} - \hat{S}_{lj} \delta_{mi} \quad (22)$$

By using the hint in section (2) the Hamiltonian (21) reduced to

$$\hat{H} = \omega_1 \hat{S}_{11} + \omega_2 \hat{S}_{22} + \sum_{j=1}^3 \Omega_j \hat{n}_1 + \Omega_2 \hat{P} + \Omega_3 \hat{Q} + \lambda(\hat{S}_{12} \hat{\zeta}^k + \hat{\zeta}^{\dagger k} \hat{S}_{21}) \quad (23)$$

where  $\hat{\zeta} = \hat{a}_1 \hat{a}_2 \hat{a}_3$ . In this case the equations of motion for the operators  $\hat{n}_1 = \hat{a}_1^\dagger \hat{a}_1$  and  $\hat{S}_{jj}$  ( $j = 1, 2$ ) are given by

$$i \frac{d\hat{n}_j}{dt} = ik \frac{d\hat{S}_{22}}{dt} = -ik \frac{d\hat{S}_{11}}{dt} = \lambda(\hat{\zeta}^{\dagger k} \hat{S}_{21} - \hat{S}_{12} \hat{\zeta}^k), \quad j = 1, 2, 3 \quad (24)$$

from which we can establish that the following operator

$$\hat{N} = \hat{n}_1 + \frac{k}{2}(\hat{S}_{11} - \hat{S}_{22}) \quad (25)$$

is a constant of motion We notice that the operators  $\hat{P}$  and  $\hat{Q}$  are also constants of motion. Using equation (24) we can cast the Hamiltonian (23), as follows

$$\hat{H} = \frac{1}{2}(\omega_1 + \omega_2)\hat{I} + \Omega_2 \hat{P} + \Omega_3 \hat{Q} + \sum_{j=1}^3 \Omega_j \hat{N} + \hat{C}. \quad (26)$$

where  $\hat{I}$  is the identity operator while  $\hat{C}$  is given by

$$\hat{C} = \frac{\Delta}{2}(\hat{S}_{11} - \hat{S}_{22}) + i\lambda(\hat{\xi}^{\dagger k}\hat{S}_{21} - \hat{S}_{12}\hat{\xi}^k). \tag{27}$$

with  $\Delta$  the detuning parameter given by

$$\Delta = \omega_1 - \omega_2 - k(\Omega_1 + \Omega_2 + \Omega_3) \tag{28}$$

It is easy to show that the operators  $\hat{N}$ ,  $\hat{P}$ ,  $\hat{Q}$ , and  $\hat{C}$  commute with each other and hence each of them commute with  $\hat{H}$ . This means that the operators  $\hat{N}$  and  $\hat{C}$  are also constants of motion.

The time evolution operator  $\hat{U}(t)$  is defined by

$$\hat{U}(t) = \exp[-i\hat{H}t]$$

By using the commuting operator  $\hat{N}$ ,  $\hat{P}$ ,  $\hat{Q}$  and  $\hat{C}$ , we can cast  $\hat{U}(t)$  in the following form

$$\begin{aligned} \hat{U}(t) = \exp\left[-\frac{i(\omega_1 + \omega_2)t}{2}\right] \exp\left[-i\sum_{j=1}^3 \Omega_j \hat{N}t\right] \\ \exp[-i\Omega_2 \hat{P}t] \exp[-i\Omega_3 \hat{Q}t] \exp[-i\hat{C}t], \end{aligned} \tag{29}$$

It is easy to show that

$$\exp\left[-i\sum_{j=1}^3 \Omega_j \hat{N}t\right] \exp[-i\Omega_2 \hat{P}t] \exp[-i\Omega_3 \hat{Q}t] = \begin{bmatrix} \exp[-i\hat{Z}_1t] & 0 \\ 0 & \exp[-i\hat{Z}_2t] \end{bmatrix}, \tag{30}$$

with

$$\hat{Z}_1 = \sum_{j=1}^3 \Omega_j \left(\hat{n}_j + \frac{k}{2}\right), \tag{31}$$

$$\hat{Z}_2 = \sum_{j=1}^3 \Omega_j \left(\hat{n}_j - \frac{k}{2}\right) \tag{32}$$

and

$$\begin{aligned} & \exp[-i\hat{C}t] \\ &= \begin{bmatrix} \left(\cos \hat{\mu}_1(\hat{n}_1)t - \frac{i\Delta}{2\mu_1(\hat{n}_1)} \sin \hat{\mu}_1(\hat{n}_1)t\right) & -i\lambda\hat{\xi}^{\dagger k} \frac{\sin \hat{\mu}_1(\hat{n}_1)t}{\hat{\mu}_1(\hat{n}_1)} \\ -i\lambda \frac{\sin \hat{\mu}_1(\hat{n}_1)t}{\hat{\mu}_1(\hat{n}_1)} \hat{\xi}^k & \left(\cos \hat{\mu}_2(\hat{n}_1)t + \frac{i\Delta}{2\mu_2(\hat{n}_1)} \sin \hat{\mu}_2(\hat{n}_1)t\right) \end{bmatrix}, \end{aligned} \tag{33}$$

with

$$\begin{aligned} \mu_j^2(\hat{n}_1) &= \frac{\Delta^2}{4} + \nu_j, \quad j = 1, 2 \\ \hat{\nu}_1(\hat{n}_1) &= \lambda^2 \frac{(\hat{n}_1 + k)! (\hat{n}_1 + \hat{P} + k)! (\hat{n}_1 + \hat{Q} + k)!}{\hat{n}_1! (\hat{n}_1 + \hat{P})! (\hat{n}_1 + \hat{Q})!}, \\ \hat{\nu}_2(\hat{n}_1) &= \lambda^2 \frac{\hat{n}_1! (\hat{n}_1 + \hat{P})! (\hat{n}_1 + \hat{Q})!}{(\hat{n}_1 - k)! (\hat{n}_1 + \hat{P} - k)! (\hat{n}_1 + \hat{Q} - k)!} = \hat{\nu}_1(\hat{n}_1 - k), \end{aligned} \quad (34)$$

where the parameter  $\mu_j(\hat{n}_1)$ ,  $j = 1, 2$  may be considered as generalized Rabi frequencies.

Now let us consider the coherent atomic state  $|\theta, \phi\rangle$  for the effective two-level atom in the following form

$$|\theta, \phi\rangle = \cos(\theta/2)|e\rangle + \sin(\theta/2)\exp(-i\phi)|g\rangle, \quad (35)$$

which acquires both excited state  $|e\rangle$  and ground state  $|g\rangle$  where  $\theta$  is the coherence angle and  $\phi$  is the relative phase of the two atomic levels. To reach the excited state we have to take  $\theta \rightarrow 0$  while to describe the particle in the ground state we have to let  $\theta \rightarrow \pi$ . For the wave function of the field we consider the generalized trio-coherent state given by Equation (11). Therefore the initial state of the system is given by  $|\psi(0)\rangle = |\zeta, p, q, k\rangle_j \otimes |\theta, \phi\rangle$  Therefore, after some calculations, neglecting the phase factor  $\exp\left[-\frac{i(\omega_1+\omega_2)t}{2}\right]$  the wave function for the system at any time  $t > 0$  takes the following form:

$$\begin{aligned} |\psi(t)\rangle &= \hat{U}(t)|\psi(0)\rangle = \left\{ \exp\{-i\hat{Z}_1t\} \left( \cos \hat{\mu}_1t - \frac{i\Delta}{2\mu_1} \sin \hat{\mu}_1t \right) \cos \frac{\theta}{2} \right. \\ &\quad \left. - i\lambda \exp\{-i\hat{Z}_1t\} \frac{\sin \hat{\mu}_1t}{\mu_1} \hat{\zeta}^k \exp\{-i\phi\} \sin \frac{\theta}{2} \right\} |\zeta, p, q, e\rangle \\ &\quad + \left\{ \exp\{-i\hat{Z}_2t\} \left( \cos \hat{\mu}_2t - \frac{i\Delta}{2\mu_2} \sin \hat{\mu}_2t \right) \exp\{-i\phi\} \sin \frac{\theta}{2} \right. \\ &\quad \left. - i\lambda \exp\{-i\hat{Z}_2t\} \frac{\sin \hat{\mu}_2t}{\mu_2} \hat{\zeta}^{\dagger k} \cos \frac{\theta}{2} \right\} |\zeta, p, q, g\rangle, \end{aligned} \quad (36)$$

with the wave function calculated, any phenomenon related to the atom and the field can be computed.

### 7. SUB-POISSONIAN DISTRIBUTION

In figure (6), the second-order correlation function  $g_1^2(0)$  for mode 1, is plotted against the scaled time  $\lambda t$ , the field is considered to be initially in a correlated trio-coherent state for  $q = 0, p = 2$ , the correlation parameter  $\zeta = 3$  and  $k = 3$  (i.e.,

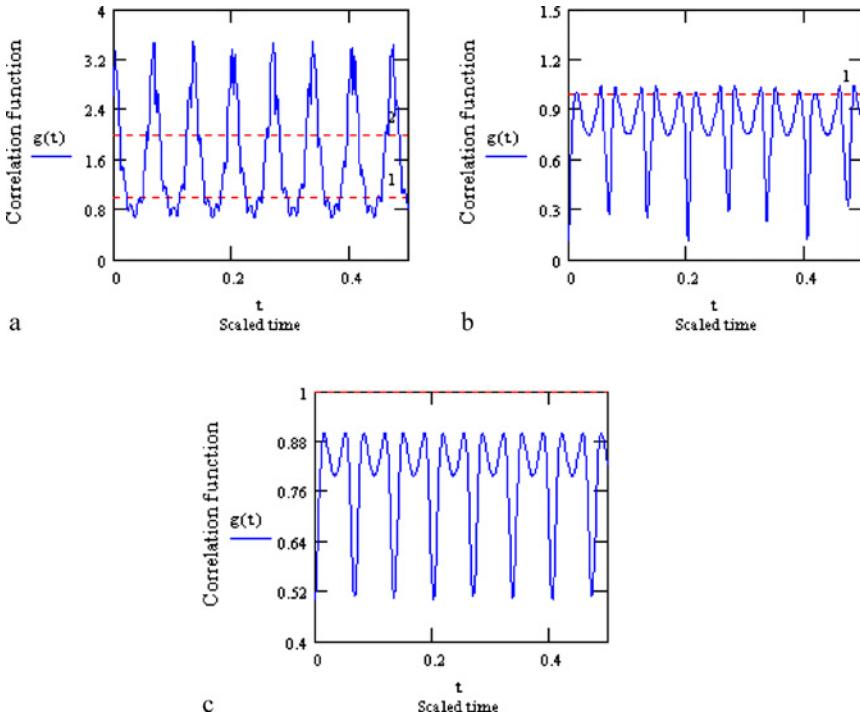


**Fig. 6.** Time evolution of the sub-Poissonian distribution  $g_1^2(t)$  against time  $\lambda t$  the atom initially in excited state ( $\theta = 0$ ) and the field is prepared in correlated trio-coherent state with parameters ( $q = 0, p = 2, \zeta = 3$ ). (a)  $j = 0$ , (b)  $j = 1$ , (c)  $j = 2$ .

$j = 0, 1, 2$ ) and the atom started from the excited state. We note that the function  $g_1^2(t)$  has oscillatory behavior in general for both cases of the atom. In Fig. 6(a) we take  $j = 0$ , the behavior of  $g_1^2(t)$  starts as super-Poissonian and thermal state as seen in the figure, we observe that the function  $g_1^2(t)$  becomes  $< 1$  thus given sub-Poissonian behavior for a short time see Fig. 6(a). The behavior is periodical. In Fig. 6(b) we take  $j = 1$  and the other parameters are the same as the previous case, the situation is changed the behavior of the function  $g_1^2(t)$  is almost sub-Poissonian and we find super-Poissonian for short intervals. While for the case  $j = 2$  and the other parameters as in the first case the behavior of the function  $g_1^2(t)$  is fully sub-Poissonian as observed in Fig. 6(c). Once again we note the periodicity.

### 8. CAUCHY-SCHWARZ INEQUALITY VIOLATION

In this subsection we shall discuss another example of the nonclassical properties for the present system. Our aim is to consider the temporal behavior of the

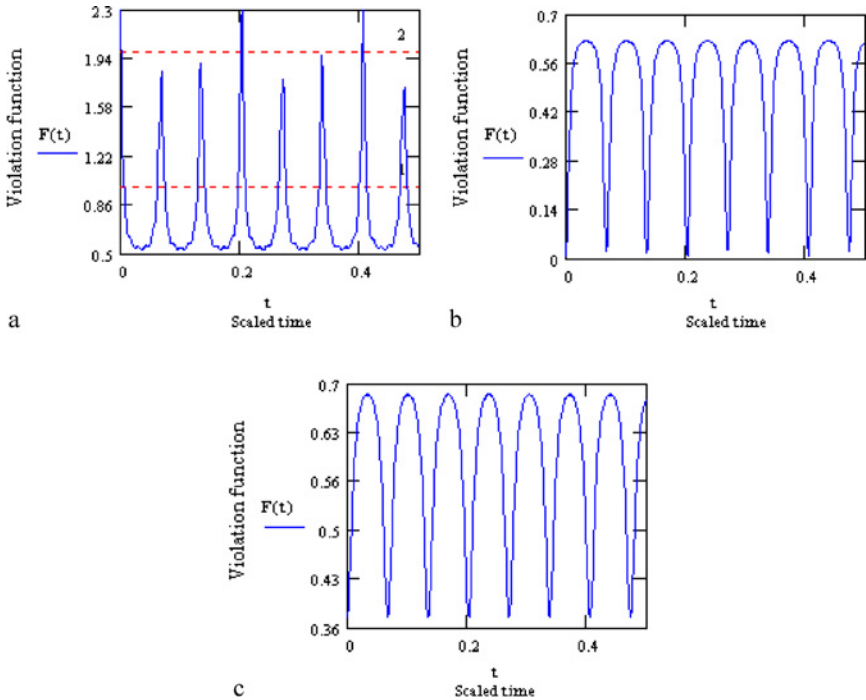


**Fig. 7.** Time evolution of the violation function  $F_{12}(t)$  against time  $\lambda t$  the atom initially in excited state ( $\theta = 0$ ) and the field is prepared in correlated trio-coherent state with parameters ( $q = 0, p = 3, \zeta = 3$ ). (a)  $j = 0$ , (b)  $j = 1$ , (c)  $j = 2$ .

violation of Cauchy-Schwarz inequality. In figure (7), the violation function  $F_{12}(t)$  for mode pair (1,2), is plotted against the scaled time  $\lambda t$ , the field is considered to be initially in a correlated trio-coherent state for  $q = 0, p = 2$ , the correlation parameter  $\zeta = 2$  and  $k = 3$  (i.e.,  $j = 0, 1, 2$ ) and the atom started from the excited state. First for  $j = 0$  the function  $F_{12}(t)$  fluctuates between partial violation and full violation as appearing in Fig. 7(a). The violation behavior is changed when we take  $j = 1, 2$ . In the two Fig. 7(c) and (d) the function  $F_{12}(t)$  is in full violation of the inequality and we see regular fluctuations. This phenomenon repeats itself periodically over of the considered time. Moreover the function  $F_{12}(t)$  when  $j = 2$  dos not reach to zero but when  $j = 1$  almost reaches the value zero.

## 9. CONCLUSION

In this work we have introduced a new class of nonclassical states, which are refereed as generalized trio coherent states. Mathematically, these states are



simultaneous eigenstates of powers of the operator that annihilates photons in trios and the operators that give the relative occupation numbers in pairs of the three modes. Physically, the GTCS can be produced by processes in which there is a strong competition between a trio parametric conversion, trio absorption and the state appears when the system reaches a stationary regime in the long-time limit of the competition. The GTCSs can be applied to any kind of boson field by using three modes. We have considered some statistical properties of these states. For example, we have considered the Glauber second-order correlation function  $g^2(0)$ , which shows that the states at  $j = 0$  is partially nonclassical for any values of  $p, q$ . At  $j \geq 1$ , on the other hand, is fully nonclassical over the whole range of  $|\zeta|$  for any values of  $p, q$ . The violation of Cauchy-Schwarz inequalities has been studied in detail. We found the violation depend sensitively on  $k$  i.e ( $j = 0, 1, 2$ ), and the parameters  $p$  and  $q$ . Finally phase properties distribution in the Pegg-Barnett approach applied to GTCS showed that it has three central completed peak. Finally, the interaction of the radiation field prepared in generalized trio coherent states with atom in the superposition coherent state in rotating wave approximation (RWA) is considered. The time dependence of the sub-Poissonian distribution, violation of Cauchy-Schwarz inequalities and the phase distribution are studied. Last but not least one might introduce generalized states that would depend on annihilation of photons in large numbers (four, five and so on). We would expect that as novel nonclassical states, GTCS, could find real implementation in the future particularly in connection with the emergence of quantum information processing (Raginsky and Knmar, 2001; Gorbachev *et al.*, 2002).

## REFERENCES

- Barnett, S. M. and Pegg, D. T. (1989). *Journal of Modern Optics* **36**, 7.
- Bhaumik, D., Bhaumik, K., and Dutta-Roy, B. (1976). *Journal of Physics A: Mathematical and General* **9**, 1507; Agrawal, G. S. (1988). *Journal of the Optical Society of America B* **5**, 1940.
- Buzek, V. and Knight, P. L. (1995). *Progress in Optics*, E. Wolf, ed., Noth-Holland, Amsterdam, **34**, P. 1–158).
- Dodonov, V. V., Malkin, I. A., and Manko, V. I. (1974). *Physica* **72**, 597.
- Gerry, C. C. and Grobe, R. (1995). *Physical Review A* **51**, 1698.
- Glauber, R. J. (1963). *Physical Review* **131**, 2766.
- Gorbachev, V. N., Zhiliba, A. I., and Trubilko, A. I. (2002). *J. Opt. B: Quan. Semi. Opt.* **3**, S25.
- Hillery, M. (1987). *Physical Review A* **36**, 3796.
- Loundon, R. (1983). *The Quantum theory of light*, Clarendon Press, Oxford.
- Nguyen, B. A. (2002). *J. Opt. B.: Quan. Semi. Opt.* **4**, 222.
- Nguyen, B. A. and Truong, M. D. (2002). *J. Opt. B.: Quan. Semi. Opt.* **4**, 80.
- Nguyen, B. A. and Truong, M. D. (2002). *J. Opt. B.: Quan. Semi. Opt.* **4**, 289.
- Pegg, D. T. and Barnett, S. M. (1988). *European Physics Letters* **6**, 483.
- Pegg, D. T. and Barnett, S. M. (1997). *Quantum Optics* **2**, 225.
- Raginsky, M. and Knmar, P. (2001). *J. Opt. B: Quan. Semi. Opt.* **3**, L1.
- Remoe, G., Schmidt-Kaler, F., and Walther, H. (1990). *Physical Review Letters A* **293**, 2783.

- Special issue on (1993). "Quantum phase and phase dependent measurements" of *Physica Scripta T* 48s, 1–142; Lynch, R. (1995). *Phys. Rep.* **256**, 367; Perinova, V., Luks, A., and Perina, J. (1998). *Phase in Optics* World Scient, Singapore.
- Xia, Y. J. and Guo, G. C. (1989). *Physics Letters A* **136**, 281.
- Yamamoto, Y. and Machida, S. (1987). *Physical Review A* **35**, 5114.
- Yi, H. S., Nguyen, B. A., and Kim, J. (2004). quant-ph/0409103 v1 16.
- Yoo, H.-I. and Eberly, J. H. (1985). *Physics Reports* **118**, 239; Bogolubov, N. N., Kien, F. L., and Shumovsky, A. S. (1984). *Physics Letters, A* **101**, 201.
- Yurke, B. and Stoler, D. (1986). *Physical Review Letters* **57**, 13.